Synthesis and cation-mediated electron transfer in intramolecular fluorescence quenching of donor–acceptor podands: observation of Marcus inverted region in forward electron transfer reactions

Hua Jiang, Huijun Xu *† and Jianping Ye

Laboratory of Photochemistry, Center of Molecular Science, Institute of Chemistry, Chinese Academy of Sciences, Beijing, P. R. China

Received (in Cambridge, UK) 18th January 2000, Accepted 2nd March 2000

The synthesis of a series of donor–acceptor podands is described. The dependence of the rate constants of intramolecular photoinduced electron transfer on the exothermicity of the reaction was studied by stationary and time-resolved fluorescence spectroscopy. ^{1}H NMR and computational studies suggest that the conformational change of the podands is restricted by K^+ binding. As a result, the occurrence of highly exothermic photoinduced electron transfer reaction within the Marcus inverted region was observed.

Introduction

Photoinduced electron transfer (PET) has been intensively studied in an attempt to understand the primary process in the natural photosynthesis of green plants and bacteria.[1] Many different D–A (donor–acceptor) systems, linked by either flexible[2] or rigid[3,4] spacers, have been designed for this purpose. For a given D–A system, the rate of PET depends on the D–A distance and relative orientation of the chromophores. For studies of this dependence, rigid dyads are generally used.[3–9] In contrast, if the spacer binding the chromophores is flexible, large conformational changes can occur following PET. Hence, the system usually exhibits more complicated behavior.

A pronounced feature of the well-known classical electron transfer theory, which was proposed by Marcus,[10] was the prediction of the existence of a so-called inverted region, where the rate constant of the ET reaction decreases with increasing free energy change ($-\Delta G$) of the reaction. No experimental evidence had been reported until quite recently. Miller *et al.*[5] first reported the observation of the inverted region on ET in bifunctional steroids between a radical anion produced by pulse radiolysis and various quinone moieties. However, the studies involved only charge-shift reactions but not photoinduced charge separation reactions. Thereafter several groups reported that in the case of D–A species, the back ET reactions occur in the Marcus inverted region.[11]

In the present investigation an attempt was made to develop a supramolecular system based on host–guest complexation driven by non-covalent interaction, which brought us to prepare a series of long chain podands **2**–**7**. Despite the fact that the donor is not rigidly connected to the acceptors, the distance and orientation between the two chromophores are restricted by cation-induced complexation. The dependence of the rate constant of PET on the exothermicity of the reactions is studied by stationary and time-resolved fluorescence spectroscopy.

Results and discussion

Synthesis

The synthesis of 2-halomethyl-9,10-dimethoxyanthracene can be carried out by two routes (Scheme 1). Anthraquinone

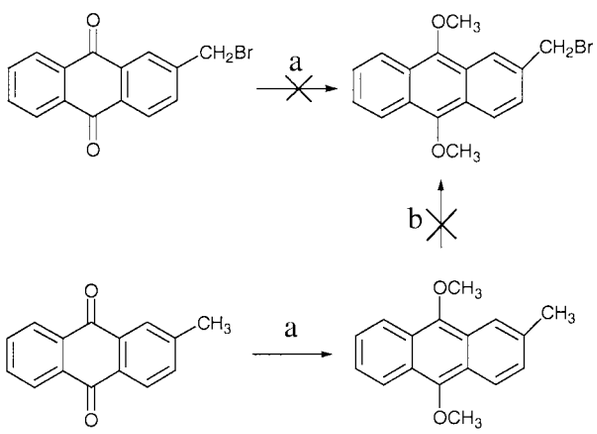

Scheme 1 *Reagents and conditions*: a: i) $Na_2S_2O_4$, H_2O and THF, ii) NaOH, H_2O, CH_3I; b: NBS, CCl_4.

was reduced by sodium dithionite in water to generate 9,10-dihydroxyanthracene as an intermediate, which was deprotonated by NaOH, followed by methylation using methyl iodide to obtain 9,10-dimethoxyanthracene in a satisfactory yield. It occurred to us that the reduction of 2-bromomethylanthraquinone under similar conditions could also give 2-bromomethyl-9,10-dimethoxyanthracene in good yield. Surprisingly, we obtained the desired product in very low yield. It was found that the intermediate 2-bromomethyl-9,10-dihydroxyanthracene can be alkylated by itself as well as by methyl iodide, which obviously decreases the yield. In order to avoid this, 2-methylanthraquinone instead of 2-halomethylanthraquinone was reduced and methylated to give 2-methyl-9,10-dimethoxyanthracene, which was then brominated by NBS in CCl_4. However, this gave 2-methylanthraquinone rather than 2-bromomethyl-9,10-dimethoxyanthracene. It is believed that oxidation probably took place in this case. We can find no reports of similar reactions. The mechanism is not clear and is worth further investigation.

Thus, we used 2-hydroxymethylanthraquinone as precursor, which was reduced by sodium dithionite and methylated using methyl iodide. The 2-hydroxymethyl-9,10-dimethoxyanthracene thus obtained was then treated with thionyl chloride in chloroform to give 2-chloromethyl-9,10-dimethoxyanthracene in good yield (Scheme 2).

Kemp has reported the hydrolysis of 2-bromomethylanthraquinone to obtain 2-hydroxymethylanthraquinone.[12,13]

† *Present address*: Institute of Photographic Chemistry, Bei-Sha-Tan, Beijing 100101, P. R. China. E-mail: g201@ipc.ac.cn. Fax: 86-10-64879375.

DOI: 10.1039/b000541j

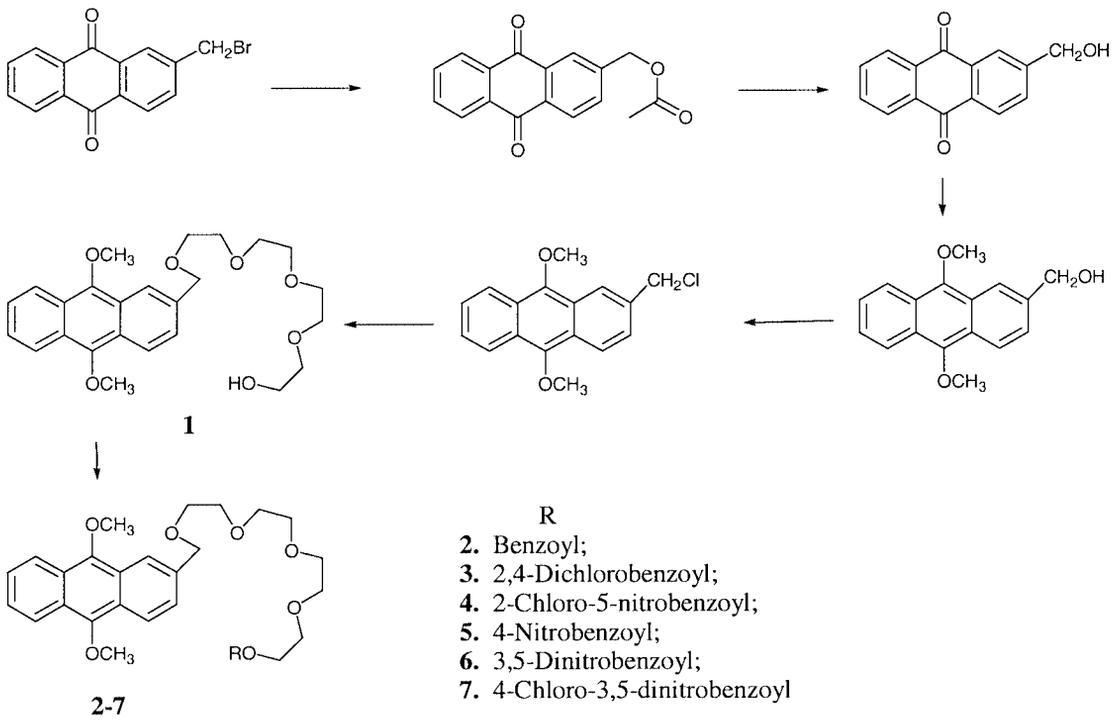

Scheme 2

However, in our system the yield of hydrolysis was low. Another reaction path was developed as shown in Scheme 2, in which 2-bromomethylanthraquinone was esterified to obtain 2-acyloxymethylanthraquinone, followed by hydrolysis to give 2-hydroxymethylanthraquinone in satisfactory yield.

UV-vis and steady-state fluorescence spectra

UV-vis studies of **2**–**7** and their cation-complexes show no ground state interaction between the donor and the acceptors. Fluorescence spectra of **3**–**7** demonstrate rapid and efficient quenching of the 9,10–dimethoxyanthracene S_1 excited state by the pendent benzoate. The intensity of fluorescence decreases successively with increasing redox potential of the pendent electron acceptor. The fluorescence spectra of **3**–**7** in the presence of K^+ also show pronounced quenching. Interestingly, the intensity of the fluorescence decreases in the order of **3** > **4** > **5**, and then increases in the order of **5** < **6** < **7** as the potential of the pendent acceptor increases (Fig. 1). The fluorescence spectra of the podands in the presence of Na^+ are no different to those of free podands.

Since no energy transfer from the donor to the acceptor is possible, the decrease of intensity of fluorescence was attributed to intramolecular PET. A deeper insight into the PET reaction can be obtained from the fluorescence decay data (Table 1). The lifetime of 15.5 ± 0.5 ns of the model compound **2** was obtained by monoexponential fit of the fluorescence decay curve. In order to get a good fit of the fluorescence decay curve of the free podands **3**–**7** double exponential functions are required. The ranges of χ^2 for all fits are 1–1.5. This indicates that the pondands exist in two conformations, *i.e.*, folded and extended conformations upon excitation (Fig. 2). The short lifetime decreases, and then remains constant with increasing redox potential, while the longer lifetimes are all the same. The short lifetime τ_1 is attributed to the deactivation of the donor excited state by intramolecular ET to the acceptor while the podand is in the folded conformation. The long lifetime τ_2 refers to the lifetime in the absence of ET while the podand is in the extended conformation.

Molecular mechanics and semiempirical calculations with the Polak–Ribiere algorithm and termination condition with RMS (Root-Mean-Square) gradient of 0.1 kcal mol^{-1} *in vacuo*

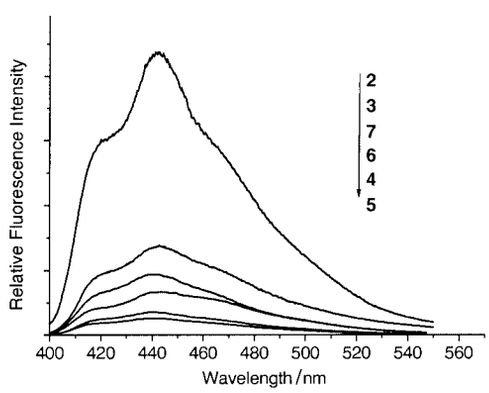

Fig. 1 Fluorescence spectra of the podands **2**–**7** in the presence of K^+ in CH_3CN. Excitation at 380 nm.

(Hypercube Inc. Release Hyperchem 5.02 for 95/NT Molecular Modeling System) carried out on the ground state of the free podand provide a detailed picture of its geometry (Fig. 2). For the extended conformation, the distance between the anthracene subunit to the benzoyl ester is about 18 Å (edge to edge). For the folded conformation, a center-to-center (anthracene to phenyl ring) distance of about 5 Å is found and the planes of the two macrorings are almost parallel.

The potassium ion exerts no effect on the lifetime of the model podand **2**. In the presence of potassium ions, the other podands **3**–**7** also show biexponential decay (Table 1). Use of a triexponential function did not significantly improve the fit. The short lifetimes τ_1 are similar to those of the free podands, attributed to the uncomplexed podands in folded conformation. The long lifetimes τ_2 decrease, and then increase with increasing redox potential of the acceptors. It seems that K^+ could restrict the conformational changes of the podands so that they exhibit quite different behavior in electron transfer reactions.

Effect of exothermicity on rate constant of PET in the podands

The rate constants of PET, shown in Table 3, were calculated by $k_{ET} = 1/\tau - 1/\tau_0$, where τ_0 is the observed fluorescence lifetime of the model podand **2** in the absence of electron transfer. The

Table 1 Fluorescence lifetime of podands **3**–**7** and their complexes

	Podands		Complexes	
	τ_1/ns (%)	τ_2/ns (%)	τ_1/ns (%)	τ_2/ns (%)
3	2 ± 0.1 (95.5)	15.2 ± 0.2 (4.5)	2 ± 0.1 (57)	12.5 ± 0.6 (43)
4	0.8 ± 0.05 (88)	15.3 ± 0.4 (12)	0.8 ± 0.06 (63)	9.9 ± 0.5 (37)
5	0.3 ± 0.03 (90.1)	15.1 ± 0.5 (9.9)	0.3 ± 0.02 (75)	6.5 ± 0.5 (25)
6	0.3 ± 0.01 (91.3)	15.3 ± 0.5 (8.7)	0.3 ± 0.01 (66.4)	11.6 ± 0.4 (33.6)
7	0.3 ± 0.01 (97.5)	15.2 ± 0.3 (2.5)	0.2 ± 0.02 (78)	14.9 ± 0.1 (22)

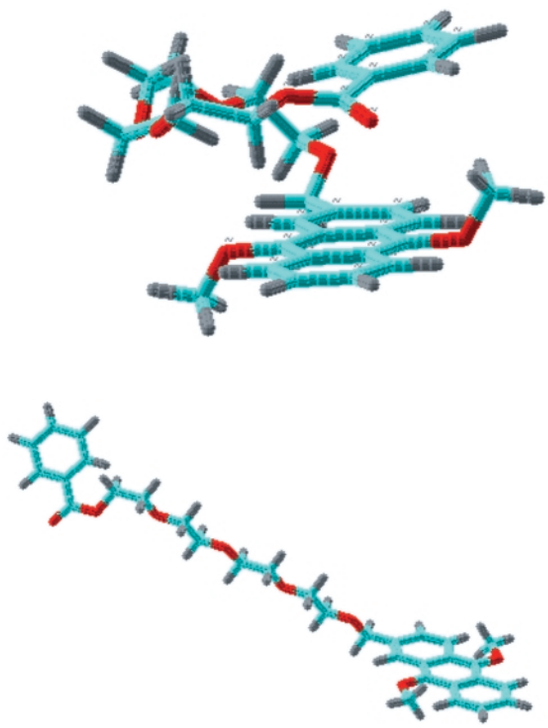

Fig. 2 AM1 geometries for **2** in its folded (top) and extended (bottom) conformations.

change of free energy of the reaction was obtained from $\Delta G = E_{O(D)} - E_{R(A)} - E_{0\text{-}0} - C$,[7–9] where $E_{O(D)}$ is the oxidation potential of the donor (Table 2), $E_{R(A)}$ is the reduction potential of acceptor, $E_{0\text{-}0}$ is the electronic excitation energy of the donor from the ground state to the first excited state and C is the coulomb interaction term, which can be neglected in this case. The rate constant of the free podands increases with increasing driving force in the normal region, until they reach the maximum, where they remain constant as the exothermicity increases (Fig. 3a). While those of the K^+-complexed podands demonstrate an increasing rate constant in the normal region, a decrease in rate constant in the highly exothermic region indicates the existence of an inverted region (Fig. 3b).

The Marcus expression of the form[10,14,15] eqn. (1), was used

$$k = A \exp\left[\frac{-(\Delta G + \lambda)^2}{4\lambda k_b T}\right] \quad (1)$$

where

$$A = \frac{2\pi}{\hbar}|H_{DA}|^2\left(\frac{1}{\sqrt{4\pi k_b \lambda T}}\right) \quad (2)$$

for a least-squares analysis of the data (Table 3). The data for each system were fitted by two free parameters, the tunneling matrix element governing the electron transfer (H_{DA}) and the reorganization energy (λ). The values obtained for **3**–**7** and their complexes are as follows: $H_{DA} = 4$ cm^{-1}, $\lambda = 1.4$ eV for

Table 2 Redox potentials (*vs.* Ag/AgCl) of substituted methyl benzoate in CH_3CN

Compounds	E_R/V
Methyl 2,4-dichlorobenzoate	−1.2
Methyl 3-chloro-5-nitrobenzoate	−0.99
Methyl 4-nitrobenzoate	−0.90
Methyl 3,5-dinitrobenzoate	−0.76
Methyl 4-chloro-3,5-dinitrobenzoate	−0.65

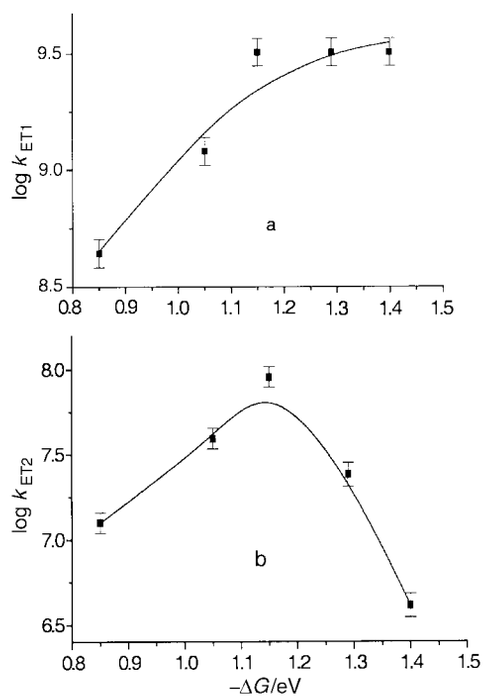

Fig. 3 Rates of PET as a function of free energy change ($-\Delta G$) in acetonitrile, a—for free podands calculated from the short lifetime component, b—for podands in the presence of K^+ calculated from the long lifetime component.

free podands **3**–**7** and $H_{DA} = 0.5$ cm^{-1}, $\lambda = 1.05$ eV for their K^+-complexes. The latter values obtained are similar to those ($H_{DA} = 0.6$ cm^{-1}, $\lambda = 1.02$ eV, unpublished results in our group) of long distance electron transfer between the 9,10-dimethoxyathracene and nitroaromatics connected by a rigid spacer.[7] In the free podands, the spacer binding the donor and acceptor is flexible, so the distance and topographic relationship of the two chromophores varies. It is believed that in this case,[5b] no diminishing rates were detected, even in the highly exothermic region. In contrast, for the podands complexed with cations (Scheme 3), the distance between the donor and acceptors is restricted, so the first-order ET rate constant can be measured without the complications of rate limiting diffusion. Hence, the decrement of rates in the highly exothermic region is observed.

The interaction of potassium ions with the podands was studied by ^{1}H NMR. Addition of a small amount of CH_3COOK to a solution of **2** in methanol-d_4–acetonitrile-d_3 (1 : 9) produced a downfield shift (up to 20 Hz) of the oligooxa-

Table 3 Free energy changes and rate constants for PET in the podands

Podands	$-\Delta G$/eV[a]	$10^9\ k_{ET1}$[b]/s^{-1}	$10^7\ k_{ET2}$[c]/s^{-1}
3	0.85	0.44 ± 0.05	1.7 ± 0.3
4	1.05	1.2 ± 0.1	3.9 ± 0.4
5	1.15	3.2 ± 0.4	9.0 ± 0.5
6	1.29	3.2 ± 0.18	2.4 ± 0.2
7	1.40	3.2 ± 0.18	0.41 ± 0.04

[a] $E_D = 0.9$ eV, $E_{0\text{-}0} = 2.95$ eV were taken from ref. 7. [b] $k_{ET} = 1/\tau - 1/\tau_0$, calculated from the short lifetime of podands in the absence of metal ion. [c] Calculated from the long lifetime of the podands in the presence of metal ion. The uncertainty in k_{ET} is less than ±15%.

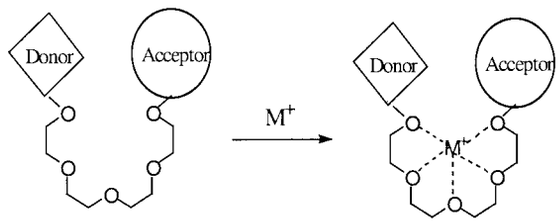

Scheme 3

ethylenic proton signals, which is consistent with that observed in the case of crown ethers and related open-chain crown ethers.[16,17] Minor shifts were observed for **2** in the presence of $NaClO_4$.

Computational studies suggest that a change in the conformation of the model podands is induced by cation binding. In the case of Na^+ the cation sits above the cavity of the pseudo crown ether, so no significant complexation with the podand could be detected. The distance between two chromophores is similar to that of free podands. In the case of complexed podands K^+ is nestled within the pseudo crown ether cavity (Fig. 4), so the distance between the 9,10-dimethoxyanthracene subunit and phenyl ring (center-to-center) is about 6 Å and the value of the dihedral angle between the two chromophores is about 55°. As a result, the distance, as well as the relative orientation, of the two chromophores is restricted, so allowing us to locate the inverted region in forward PET reactions.

Experimental

Instruments and methods

^{1}H NMR were obtained with Varian Gemini 200 or 400 spectrometers. IR were measured on a BIO-RAD FTS 165 spectrometer. Mass spectra were recorded on a Trio 2000 spectrometer. UV-Vis spectra were obtained on a UV-1601PC spectrophotometer. Fluorescence spectroscopic studies were performed on a HITACHI-F4500 with excitation at 380 nm and emission at 450 nm (with slit bandwidths of 5 nm and 2.5 nm, respectively). Fluorescence decay curves were obtained by a Horiba Time-resolved Spectrofluorometer NAES-1100 single-photon-counting apparatus. The fluorescence lifetimes were determined from data on the fluorescence transient waveform of the material to be tested and the lamp waveform data using the least squares iterative deconvolution method and can be analyzed by biexponential fits. Errors in the lifetimes are under 10%. The range of χ^2 (chi-squares) are from 1.0 to 1.5. The shortest lifetime that can be determined is 200 ps. The concentration of solution was *ca.* 1×10^{-5} M. The concentration of metal ion was 20 times of that of the free podand. Redox potentials were determined by cyclic voltammetry (EG&G 283) with a Pt electrode as the working electrode, using 0.1 M tetrabutylammoniumperchlorate as the supporting electrolyte in acetonitrile under N_2, Pt wire as counter electrode, and Ag/AgCl as reference electrode (Table 2).

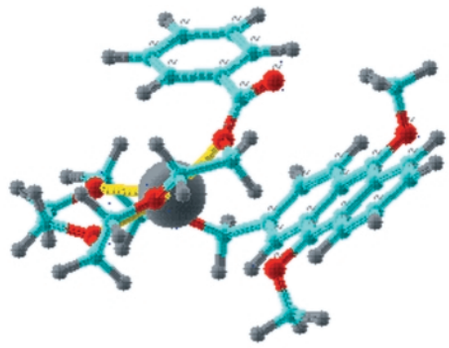

Fig. 4 Minimizing structure of K^+ + **2** complex derived from the PCMODEL calculation.

Chemicals

Due to the sensitivity of podands to light, some measurements were performed in the dark. All podands were further purified by flash chromatography before use. Acetonitrile was purified by the following procedure: acetonitrile was refluxed for 1 h with anhydrous aluminium chloride (15 g L^{-1}) and distilled, followed by reflux with $KMnO_4$ (10 g L^{-1}) and Li_2CO_3 (10 g L^{-1}), and distilled. The distillate was then refluxed with CaH_2 to remove water and distilled. Other solvents used were of reagent grade, further purified by the usual procedures.[18] 2-Methylanthraquinone was brominated by NBS to give 2-bromomethylanthraquinone according to the standard method.[19] Methyl 2,4-dichlorobenzoate, methyl 4-nitrobenzoate, methyl 3-chloro-5–nitrobenzoate, methyl 3,5-dinitrobenzoate and methyl 4-chloro-3,5-dinitrobenzoate were synthesized by known methods.[20]

Syntheses

2-Acyloxymethyl-9,10-anthraquinone.[13] To a solution of anhydrous sodium acetate (30 g) in 200 mL acetic acid and 100 mL acetic anhydride, 2-bromomethyl-9,10-anthraquinone (10 g, 33.2 mmol) was added. The reaction mixture was refluxed for 12 h, then most of the solvent was removed by distillation. The residue was cooled and poured into water, and the precipitate was collected by filter, followed by washing with water until free of acid. The crude product was purified by silica gel chromatography (eluant: benzene) to give 7 g of solid (75%), mp 147–149 °C.

2-Hydroxymethyl-9,10-anthraquinone. 2-Acyloxymethyl-9,10-anthraquinone (4 g, 14.2 mmol) were suspended in 160 mL methanol, then NaOH (0.7 g, 17.5 mmol) in 20 mL water was added. The solution was refluxed for 6 h, cooled and poured into water. The precipitate was filtered under suction, washed with water and dried *in vacuo*. The crude product was subjected to silica gel chromatography (eluant: chloroform) to give a yellow solid (3.2 g, 93%), mp 200–201 °C (lit.[12,13] mp 198–201 °C).

2-Hydroxy-9,10-dimethoxyanthracene. 2-Hydroxy-9,10-anthraquinone (5.50 g, 23.1 mmol) and tetrabutylammonium bromide (1 g) were dissolved in 60 mL THF and 250 mL water, and stirred at room temperature, followed by addition of a solution of sodium dithionite (25 g) in 50 mL water. After 2 h a solution of NaOH (22 g, 0.55 mol) in water was added, the solution immediately turned dark red. Methyl iodide (25 ml) was added, and the mixture stirred for 24 h. The mixture was extracted successively three times with 50 mL chloroform, then the extract was washed with water, and dried over anhydrous $MgSO_4$. After filtering off the $MgSO_4$, the filtrate was concentrated on a rotary evaporator. The crude product was recrystallized from toluene to give a yellow solid (4.5 g, 73%),

mp 118–120 °C. IR (KBr, ν_{max}/cm^{-1}) 3433 (OH), 2939 (-CH_3), 2872 (-OCH_3), 1635, 1450 (Ar), 1070 (C–O); ^{1}H NMR ($CDCl_3$) δ_H 8.20–8.32 (m, 4H, anthryl), 7.48–7.54 (m, 3H, anthryl), 4.75 (s, 2H, -CH_2OH), 4.12 (s, 3H, -OCH_3), 4.13 (s, 3H, -OCH_3); MS (*m*/*z*), 286(M^+).

2-Chloromethyl-9,10-dimethoxyanthracene. 2-Hydroxymethyl-9,10-dimethoxyanthracene (2.5 g, 9.3 mmol) was suspended in dry $CHCl_3$ (30 mL). The mixture was cooled below 5 °C. A solution of thionyl chloride (1.2 g, 10 mmol) in $CHCl_3$ (10 mL) was added dropwise. The reaction mixture was then stirred for 30 min. Subsequently, the solution was washed with water, dried and filtered, then the filtrate was concentrated *in vacuo*. The residue was purified by silica gel chromatography (eluant: toluene) to afford a yellow solid (2.3 g, 87%), mp 124–126 °C. IR (KBr, ν_{max}/cm^{-1}) 2935 (CH_3), 1617, 1446, 1370 (Ar), 1261, 1065 (O–C); ^{1}H NMR ($CDCl_3$) δ_H 8.24–8.35 (m, 4H, anthryl), 7.49–7.54 (m, 3H, anthryl), 4.82 (s, 2H, -CH_2Cl), 4.12 (s, 3H, -OCH_3), 4.13 (s, 3H, -OCH_3); MS (*m*/*z*), 286(M^+), 288(M^+ + 2).

2-(13-Hydroxy-2,5,8,11,-tetraoxatridecyl)-9,10-dimethoxyanthracene. NaH (0.3 g) was suspended in a solution of tetraethylene gycol (2.8 g, 14.5 mmol) in THF (50 mL) and stirred for 20 min at room temperature. The mixture was heated to reflux, and a solution of 2-chloromethyl-9,10-dimethoxyanthracene (0.85 g, 3 mmol) in THF (20 mL) was added dropwise. After that, the reaction mixture was stirred for another 4 h, then cooled. Methanol (20 mL) was added and stirred for 15 min, then filtered. The filtrate was concentrated and the residue was subjected to silica gel chromatography (eluant: ethyl acetate) to give a pale yellow oil (1.1 g, 93%). IR (KBr, ν_{max}/cm^{-1}) 3435 (OH), 2935 (CH_3), 2871 (OCH_3), 1631, 1450, 1367 (Ar), 1103, 1070 (C–O); ^{1}H NMR ($CDCl_3$) δ_H 8.20–8.29 (m, 4H, anthryl-H), 7.46–7.58 (m, 3H, anthryl-H), 4.76 (s, 2H, -OCH_2anthryl), 4.07 (s, 3H, CH_3O-), 4.08 (s, 3H, CH_3O-), 3.87 (t, J = 4.8 Hz, 2H, -C$H_2$$OCH_2$Ar), 3.61–3.70 (m, 14H, OCH_2-CH_2O); MS (*m*/*z*), 444(M^+).

General synthetic procedure for the podands 2–7

DCC (1.1 mmol), DMAP (0.1 mmol) and benzoic acid or substituted benzoic acid (1 mmol) were suspensed in CH_2Cl_2 (30 mL). A solution of 2-(13-hydroxy-2,5,8,11-tetraoxatridecyl)-9,10-dimethoxyanthracene **1** (1 mmol) was then added. The reaction mixture was stirred for 2 h at room temperature, and the mixture was then filtered. The filtrate was concentrated on a rotary evaporator. The residue was purified by chromatography on silica gel (eluant: CH_2Cl_2 and 1–3% methanol) to give an oil (yield 85–91%).

1-(9,10-Dimethoxyanthracen-2-ylmethoxy)-11-benzoyloxy-3,6,9-trioxaundecane (2). IR (KBr, ν_{max}/cm^{-1}) 2937 (CH_3), 2870 (OCH_3), 1733 (C=O), 1631, 1586, 1365 (Ar), 1286, 1243, 1102, 1069 (C–O); ^{1}H NMR (CD_3CN) δ_H 8.18–8.29 (m, 4H, anthryl-H), 7.82–8.0 (m, 5H, phenyl-H), 7.44–7.58 (m, 3H, anthryl-H), 4.73 (s, 2H, -OCH_2anthryl), 4.43 (t, J = 4.8 Hz, 2H, -CH_2OBz), 4.07 (s, 3H, CH_3O-), 4.08 (s, 3H, CH_3O-), 3.90 (t, J = 4.6 Hz, 2H, -C$H_2$$OCH_2$anthryl), 3.61–3.70 (m, 12H, OCH_2CH_2O); MS (*m*/*z*), 548(M^+).

1-(9,10-Dimethoxyanthracen-2-ylmethoxy)-11-(2′,4′-dichlorobenzoyloxy)-3,6,9-trioxaundecane (3). IR (KBr, ν_{max}/cm^{-1}) 2935 (CH_3), 2871 (OCH_3), 1735 (C=O), 1631, 1586, 1367 (Ar), 1285, 1248, 1102, 1069 (C–O); ^{1}H NMR (CD_3CN) δ_H 7.22–8.31 (m, 10H, Ar-H), 4.78 (s, 2H, -OCH_2anthryl), 4.44 (t, J = 4.6 Hz, 2H, -CH_2OBz), 4.11 (s, 3H, CH_3O-), 4.12 (s, 3H, CH_3O-), 3.80 (t, J = 4.4 Hz, 2H, -C$H_2$$OCH_2$anthryl), 3.68–3.72 (m, 12H, OCH_2CH_2O); MS (*m*/*z*), 617 (M^+), 619 (M^+ + 2), 621 (M^+ + 4).

1-(9,10-Dimethoxyanthracen-2-ylmethoxy)-11-(2′-chloro-5′-nitrobenzoyloxy)-3,6,9-trioxaundecane (4). IR (KBr, ν_{max}/cm^{-1}) 2933 (CH_3), 2865 (OCH_3), 1734 (C=O), 1638, 1586, 1366 (Ar), 1348 (NO_2), 1280, 1245, 1102, 1070 (C–O); ^{1}H NMR (CD_3CN) δ_H 8.66 (d, $J_{4,6}$ = 2 Hz,1H, phenyl), 8.19–8.30 (m, 5H, Ar-H), 7.47–7.60 (m, 4H, Ar-H), 4.78 (s, 2H, -OCH_2anthryl), 4.55 (t, J = 4.8 Hz, 2H, -CH_2OBz), 4.11 (s, 3H, CH_3O-), 4.12 (s, 3H, CH_3O-), 3.81 (t, J = 4.6 Hz, 2H, -C$H_2$$OCH_2$anthryl), 3.70–3.72 (m, 12H, OCH_2CH_2O); MS (*m*/*z*), 627(M^+), 629(M^+ + 2).

1-(9,10-Dimethoxyanthracen-2-ylmethoxy)-11-(4′-nitrobenzoyloxy)-3,6,9-trioxaundecane (5). IR (KBr, ν_{max}/cm^{-1}) 2940 (CH_3), 2871 (OCH_3), 1732 (C=O), 1630, 1586, 1367 (Ar), 1350 (NO_2), 1280, 1101, 1071 (C=O); ^{1}H NMR (CD_3CN) δ_H 8.18–8.31 (m, 8H, Ar-H), 7.47–7.52 (m, 3H, Ar-H), 4.78 (s, 2H, -OCH_2anthryl), 4.50 (t, J = 4.6 Hz, 2H, -CH_2OBz), 4.11 (s, 6H, CH_3O-), 3.82 (t, J = 4.4 Hz, 2H, -C$H_2$$OCH_2$anthryl), 3.70–3.72 (m, 12H, OCH_2CH_2O); MS (*m*/*z*), 593(M^+), 594(M^+ + 1).

1-(9,10-Dimethoxyanthracen-2-ylmethoxy)-11-(3′,5′-dinitrobenzoyloxy)-3,6,9-trioxaundecane (6). IR (KBr, ν_{max}/cm^{-1}) 2939 (CH_3), 2872 (OCH_3), 1732 (C=O), 1629, 1545, 1366 (Ar), 1345 (NO_2), 1278, 1170, 1100, 1070 (C–O); ^{1}H NMR ($CDCl_3$, 400 MHz) δ_H 9.04 (s, 1H, phenyl-H), 8.95 (m, 2H, phenyl-H), 8.23–8.25 (m, 3H, anthryl-H), 8.17 (s, 1H, anthryl-H), 7.49–7.55 (m, 3H, anthryl-H), 4.82 (s, 2H, -OCH_2anthryl), 4.55 (t, J = 5 Hz, 2H, -CH_2OBz), 4.13 (s, 3H, CH_3O-), 4.12 (s, 3H, CH_3O-), 3.93 (t, J = 5 Hz, 2H, -C$H_2$$OCH_2$anthryl), 3.78–3.81 (m, 12H, OCH_2CH_2O); MS (*m*/*z*), 638(M^+), 639(M^+ + 1).

1-(9,10-Dimethoxyanthracen-2-ylmethoxy)-11-(4′-chloro-3′,5′-dinitrobenzoyloxy)-3,6,9-trioxaundecane (7). IR (KBr, ν_{max}/cm^{-1}) 2931 (CH_3), 2856 (OCH_3), 1734 (C=O), 1648, 1546, 1367 (Ar), 1348 (NO_2), 1283, 1167, 1102, 1069 (C–O); ^{1}H NMR ($CDCl_3$) δ_H 8.50 (s, 2H, phenyl-H), 8.16–8.27 (m, 4H, anthryl-H), 7.45–7.52 (m, 3H, anthryl-H), 4.77 (s, 2H, -OCH_2anthryl), 4.44 (t, J = 4.8 Hz, 2H, -CH_2OBz), 4.10 (s, 3H, CH_3O-), 4.09 (s, 3H, CH_3O-), 3.78 (t, J = 5 Hz, 2H, -C$H_2$$OCH_2$anthryl), 3.67–3.72 (m, 12H, OCH_2CH_2O); MS (*m*/*z*), 672(M^+), 674(M^+ + 2).

Conclusion

By altering the relative spatial disposition of the donor and acceptor in the podands, the intramolecular PET reaction can be influenced. A decrease of the PET rate in the highly exothermic region is observed for podands with cation binding, consistent with the prediction by Marcus. In contrast, the PET rate constant was found to retain its value, equivalent to the diffusion-limited rate, throughout this region, similar to the Rehm–Weller behavior in the free podands.

Acknowledgements

We are grateful to the National Science Foundation of China for the support of this work (Grant No. 29733100).

References

1 J. S. Connolly and J. R. Ballon, in *Photoinduced Electron Transfer*, eds. M. A. Fox and M. Chanon, Elsevier, Amsterdam, 1988, Part D, p. 303; M. R. Wasielewski, *Chem. Rev.*, 1992, **92**, 435.
2 T. Ganduly, D. K. Sharama, S. Gauthier, D. Gravel and G. Durocher, *J. Phys. Chem.*, 1992, **96**, 3757.
3 J. Kroon, H. Oevering, J. W. Verhoeven, J. M. Warman, A. M. Oliver and M. N. Paddon-Row, *J. Phys. Chem.*, 1993, **97**, 5065.
4 K. D. Jordon and M. N. Paddon-Row, *Chem. Rev.*, 1992, **92**, 395.
5 (*a*) J. R. Miller, L. T. Calcaterra and G. L. Closs, *J. Am. Chem. Soc.*, 1984, **106**, 3047; (*b*) J. R. Miller, J. V. Beitz and R. K. Huddleston, *J. Am. Chem. Soc.*, 1984. **106**, 5057.
6 A. D. Joran, B. A. Leland, P. M. Felker, A. H. Zwail, J. J. Hopfield and P. B. Dervan, *Nature*, 1987, **327**, 50.

7 S. Z. Zhou, S. Y. Shen, Q. F. Zhou and H. J. Xu, *J. Chem. Soc., Chem. Commun.*, 1992. **9**, 669.
8 G. Kab, T. Engel, H. Laning and F. W. Scheider, *Ber. Bunsenges. Phys. Chem.*, 1995, **99**, 118.
9 S. Sinha, R. De and T. Ganguly, *J. Phys. Chem.*, *A*, 1997, **101**, 2852.
10 (*a*) R. A. Marcus, *J. Phys. Chem.*, 1956, **24**, 966; (*b*) R. A. Marcus, *J. Phys. Chem.*, 1956, **24**, 979; (*c*) R. A. Marcus, *J. Phys. Chem.*, 1957, **26**, 867.
11 (*a*) M. R. Wasielewski, M. P. Niemczy, W. A. Svec and E. B. Pewitt, *J. Am. Chem. Soc.*, 1985, **107**, 1980; (*b*) N. Matoga, N. H. Shioyama and Y. Kanda, *J. Phys. Chem.*, 1987, **91**, 314; (*c*) I. R.Gould and S. Farid, *J. Phys. Chem.*, 1992, **96**, 7635.
12 *Reagents for Organic Synthesis*, Wiley, 1967–78, **8**, 252.
13 D.S. Kemp, *Tetrahedron Lett.*, 1977, 1031.
14 J. Hopfield, *J. Proc. Natl. Acad. Sci. USA*, 1974, **71**, 3640.
15 R. A. Marcus and N. Sutin, *Biochem. Biophys. Acta.*, 1985, **811**, 265.
16 D. Monti, M. Venanzi and G. Mancini, *Eur. J. Org. Chem.*, 1999, 1901.
17 P. S. Baran, R. R. Monaco, A. U. Khan, D. L. Schuster and S. R. Wilson, *.J. Am. Chem. Soc.*, 1997, **119**, 8363.
18 D. D. Perrin and W. L. F. Armarego, *Purification of Laboratory Chemicals*, Pergamon, Oxford, 1980.
19 A.I. Vogel, *Practical Organic Chemistry*, 1956, 701.
20 S. L. Li, Dissertation of Institute of Photographic Chemistry, Chinese Academy of Science, 1997.